Synthesis and X-ray Characterization of Alkoxy-Substituted Aromatic Polyesters Containing Terphenyl or Quinquephenyl Units in the Main Chain

F. Kakali,[†] J. Kallitsis,[†] T. Pakula,*[,‡,§] and G. Wegner[‡]

Department of Chemistry, University of Patras, 26500 Patras, Greece, and Max-Planck-Institut für Polymerforschung, Postfach 3148, 55021 Mainz, Germany

Received March 17, 1998; Revised Manuscript Received June 29, 1998

ABSTRACT: Soluble aromatic polyesters derived from 2′,5′-dialkoxy-*p*-terphenyl-4,4′-diols or 2″,5″-didodecyloxy-*p*-quinquephenyl-4,4‴-diol and terephthaloyl or 2,5-dialkoxy-terephthaloyl dichlorides were prepared. The polymers were characterized by viscosimetry, thermal analysis, and X-ray diffraction. The polyesters show two or more endothermic transitions. The high-temperature transitions to an isotropic melt moved to lower temperatures as the side chain length increased. Structural information was obtained from the temperature-dependent X-ray data. Various structures were observed depending on the type of the phenylene segment in the backbone, the length of alkoxy side chains, and the number of side chains per backbone repeat unit.

Introduction

Substituted rigid polymers have received much attention because of substituent effects on solubility as well as on the formation of layered mesophases.[1] Polymers with substituents such as alkyl,[2−3] alkoxy,[4−7] and phenyl[8−10] have been made, but only polymers bearing alkoxy groups have been extensively studied.[4−7,11,12] Most of these studies were concerned with substituted polymers with a poly(*p*-phenylene terephthalate) backbone. Because of the effective decrease of the transition temperatures caused by the attachment of alkoxy side chains, these processable polymers did not exhibit a sufficiently high modulus at temperatures above 150 °C.[7,11]

An approach to increase the rigidity, particularly at high temperatures, consists of introduction of oligophenyl segments into the polymer backbone.[13−18] Such polymers bearing alkyl[13,14] or phenyl[15−18] side groups show increased solubility and high modulus at high temperatures; however, they did not show liquid crystallinity. Contrary to that, alkoxy-substituted polyesters containing terphenyl units in the main chain exhibited a different thermal behavior.[16]

To explore the influence of the size of the alkoxy side chain, as well as of the oligophenyl segment length in the main chain, on the order−disorder phenomena, alkoxy-substituted polyesters having the terphenyl or the quinquephenyl segments in the backbone have been synthesized. These structures may be compared with similar alkoxy-substituted poly(*p*-phenylene terephthalate)s, which have been examined in detail by X-ray.[1,4,6,11] Generally, two modifications have been observed, which were related to different modes of organization of the side chains. They were termed A and B. Both modifications are layered structures, however, in one case with side chains normal to the backbone layer (A) and in the other case with side chains titled with respect to the layers (B).

In this work, we report on the synthesis and structural characterization of aromatic polyesters bearing alkoxy side chains. Oligophenyl segments such as *p*-terphenyl or *p*-quinquephenyl were incorporated in the main chain and their influence on the polymer properties such as the solubility, microphase formation, and transition temperatures were examined.

Experimental Section

Materials. Chemicals were purchased from Aldrich and used as received. 1,4-Dibromo-2,5-bis(dodecyloxy)- and 1,4-dibromo-2,5-bis(hexadecyloxy)benzenes,[19] 2,5-bis(dodecyloxy)- and 2,5-bis(hexadecyloxy)terephthalic acids,[20] 2,5-bis(dodecyloxy)phenylene-1,4-bis(boronic acid)[21] and the catalyst dichloro[1,1′-bis(diphenylphosphino)ferrocene]palladium(II), $PdCl_2$(dppf),[22] were synthesized according to known procedures. Tetrahydrofuran was distilled from sodium in the presence of benzophenone directly into the reaction flask.

Monomer Synthesis. Reactions leading to monomers used are shown in Scheme 1. The following compounds have been synthesized and characterized:

(a) 4-Bromo-4′-(benzyloxy)biphenyl (6). A mixture of 1,4-dibromobenzene (30.0 g, 127 mmol) and $PdCl_2$(dppf) (1.023 g) was degassed, flushed with argon (3 times), dissolved in freshly distilled THF (30 mL), and heated at reflux. The solution was cooled to 0 °C and [*p*-(benzyloxy)phenyl]magnesium bromide (130 mmol) in THF was added within 40 min. The mixture was heated at reflux for 1 day under an Ar atmosphere. Quenching with diluted HCl and methanol gave a solid that was filtered and washed with methanol. Recrystallization from cyclohexane gave 28.4 g (66%) of desired product **6** (see Scheme 1), which had mp 154−156 °C. FT-IR (KBr, cm^{-1}): 3036, 1608, 1522, 1482, 1454, 1382, 1286, 1252, 1196, 1178, 1080, 1028, 998, 812, 730, 696. ^{1}H NMR (DMSO-d_6): δ 5.15 (d, 2H), 7.10 (m, 2H), 7.40 (m, 7H), 7.60 (m, 4H).

(b) 2′,5′-Bis(dodecyloxy)-*p*-terphenyl-4,4″-diol (4a). 2,5-Bis(dodecyloxy)-1,4-dibromobenzene (**1a**) (5 g, 8.28 mmol) and $PdCl_2$ (dppf) (90 mg) were degassed and flushed with argon and then dissolved in freshly dis-

[†] University of Patras.
[‡] Max-Planck-Institut für Polymerforschung.
[§] Also at the Intitute of Polymers, Technical University, Lodz, Poland.

S0024-9297(98)00413-6 CCC: $15.00 © 1998 American Chemical Society
Published on Web 08/21/1998

Scheme 1. Schemes of Reactions Used in Monomer Synthesis[a]

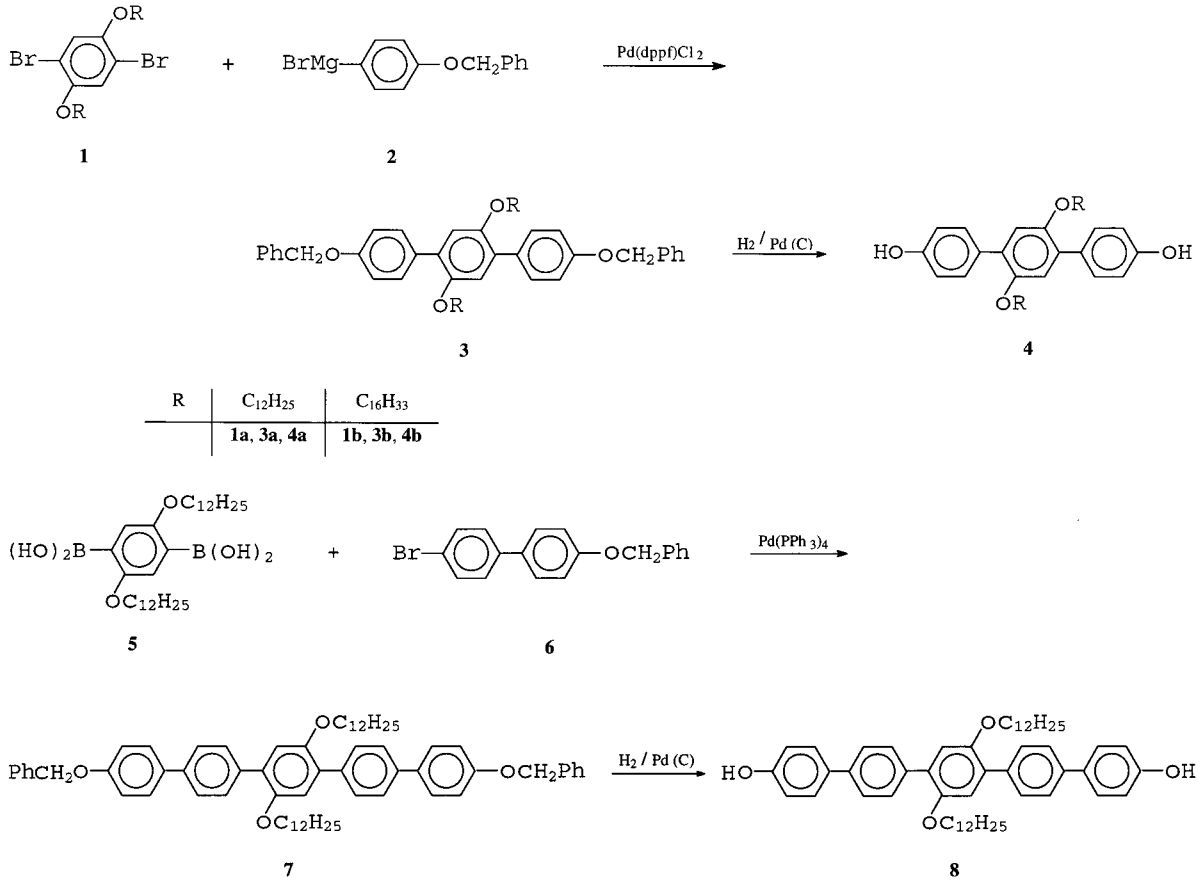

[a] All compounds are denoted by numbers used in the text. Compounds with different substituents (R) are distinguishable by means of letters a and b, according to the inserted table.

tilled THF (40 mL). The solution was cooled to room temperature and [*p*-(benzyloxy)phenyl]magnesium bromide (30 mmol) in THF was added within 30 min. The mixture was heated at reflux for 1 day and quenched with diluted HCl and methanol. The solid was isolated by filtration, washed with methanol and dried in vacuo. Recrystallization from toluene gave 5.2 g (78%) of **3a**, mp 89−90 °C. FT-IR (KBr, cm^{-1}): 2920, 2850, 1608, 1524, 1494, 1466, 1380, 1246, 1214, 1178, 1008, 1027, 810, 742, 694, 514.

3a was reduced using hydrogen and 10% Pd on activated carbon, and then recrystallization from cyclohexane gave 3.6 g (89%) of the desired diol **4a**, mp 121−122 °C. FT-IR (KBr, cm^{-1}): 3332, 2922, 2850, 1612, 1526, 1494, 1466, 1386, 1236, 1174, 1072, 832, 630. ^{1}H NMR ($CDCl_3$): δ 0.89 (t, 6H), 1.29 (m, 36H), 1.67 (m, 4H), 3.90 (t, 4H), 6.87 (d, 4H), 6.95 (s, 2H), 7.50 (d, 4H). ^{13}C NMR ($CDCl_3$): δ 14.10, 22.67, 26.05, 29.35, 29.58, 31.89, 69.60, 114.63, 114.83, 116.15, 129.96, 130.08, 130.71, 150.17, 154.80.

(c) 2′,5′-Bis(hexadecyloxy)-*p*-terphenyl-4,4″-diol (4b). 4,4″-Bis(benzyloxy)-2′,5′-bis(hexadecyloxy)-*p*-terphenyl (**3b**) was synthesized according to the procedure described for **3a**, with 85% yield and mp 76−77 °C. FT-IR (KBr, cm^{-1}): 2918, 2850, 1610, 1552, 1494, 1468, 1386, 1242, 1216, 1178, 1012, 830, 742, 694, 664.

The solid **3b** was reduced using hydrogen and 10% Pd on C and gave the desired diol **4b** with 79% yield and mp 99−100 °C. FT-IR (KBr, cm^{-1}): 3330, 2918, 2850, 1610, 1524, 1494, 1468, 1384, 1236, 1178, 836, 635. ^{1}H NMR ($CDCl_3$): δ 0.87 (t, 6H), 1.30 (m, 52H), 1.67 (m, 4H), 3.90 (t, 4H), 6.85 (s, 2H), 6.90 (d, 4H), 7.50 (d, 4H). ^{13}C NMR ($CDCl_3$): δ 14.11, 22.67, 26.05, 29.29, 29.35, 29.58, 29.68, 31.90, 69.61, 114.79, 116.71, 129.93, 130.76, 131.00, 150.17, 154.54.

(d) 2″,5″-Didodecyloxy-*p*-quinquephenyl-4,4′′′′-diol (8). 2,5-Bis(dodecyloxy) bis(boronic acid) (4.0 g, 7.5 mmol), 4-bromo-4″-(benzyloxy)biphenyl (10.2 g, 30.0 mmol) and 524 mg tetrakis(triphenylphosphine)palladium [$Pd(PPh_3)_4$] were placed together in a reaction flask. The flask was evacuated and filled with argon several times. Then 30 mL of degassed toluene and 15 mL of degassed 2 M Na_2CO_3 were added, and the mixture was heated at reflux for 48 h. The catalyst was removed by filtration and the organic phase was cooled at room temperature. The product **7** was precipitated by cooling and isolated by filtration, washed with cyclohexane and hexane, and dried in vacuo. Recrystallization from toluene gave 5.4 g (75%) of pure compound **7**, which had mp 151−153 °C. FT-IR (KBr, cm^{-1}): 2920, 2850, 1608, 1508, 1490, 1488, 1380, 1274, 1248, 1200, 1176, 1042, 822, 732, 694, 516. ^{1}H NMR ($CDCl_3$): δ 0.85 (t, 6H), 1.22 (m, 32H), 1.35 (m, 4H), 1.70 (m, 4H), 3.95 (t, 4H), 5.12 (s, 4H), 7.03 (s, 2H), 7.05 (d, 4H), 7.40 (m, 10H), 7.58 (d, 4H), 7.62 (d, 4H), 7.70 (d, 4H). ^{13}C NMR ($CDCl_3$): δ 14.10, 22.68, 26.11, 29.30, 29.36, 29.38, 29.60, 29.64, 29.68, 31.91, 69.69, 70.13, 115.18, 116.23, 126.21, 127.48, 127.98, 128.03, 128.61, 129.88, 130.41, 133.81, 136.86, 137.03, 139.26, 150.43, 158.40.

Reduction of **7** using the same system as previously reported and recrystallization from cyclohexane gave the desired product **8** with 79% yield, mp 168−170 °C. FT-IR (KBr, cm^{-1}): 3346, 2920, 2850, 1608, 1508, 1488,

Table 1. Viscosities, X-ray Data, and Thermal Analysis of the Synthesized Polyesters

					DSC (°C)					
	[η] mL/g				first heating			second heating		
polymer	30 °C	60 °C	d^b (Å)	d^c (Å)	T_1	T_2	T_3	T_1	T_2	T_3
PT12-2	*a*	148	12.6	21.5	98	165	255		218	250
PT16-2	*a*	118	25.0		90	137	210		195	222
PT12-4	27		25.2	22.1		100	~165		108	
PT16-4	31		26.7	26.7	65	105	155	65	105	155
PQ12-2(a)		40				105	148		105	148
PQ12-2(b)	*a*	175	16.6			~210	238			238
PQ12-4	37									

[a] Gellation. [b] Measured at room temperature. [c] Measured at 20 °C below the isotropization temperature.

1466, 1386, 1230, 1212, 1172, 1072, 1004, 820, 721, 521. ^{1}H NMR ($CDCl_3$): δ 0.87 (t, 6H), 1.23 (m, 32H), 1.38 (m, 4H), 1.71 (m, 4H), 3.95 (t, 4H), 4.74 (s, OH), 6.92 (d, 4H), 7.04 (s, 2H), 7.55 (d, 4H), 7.60 (d, 4H), 7.67 (d, 4H). ^{13}C NMR ($CDCl_3$): δ 14.12, 22.70, 26.12, 29.31, 29.37, 29.61, 29.65, 29.69, 31.92, 69.70, 115.67, 116.22, 126.21, 128.33, 129.89, 130.41, 133.85, 136.89, 139.25, 150.42, 155.07.

Polymer Synthesis. (a) Solution Polymerization. The aromatic polyesters bearing dialkoxy substituents in both the diol and terephthalic acid moieties were prepared by polycondensation in solution as described previously.[16]

(b) Melt Polymerization. A mixture of 1.01 mmol of the respective dialkoxy-substituted aromatic diol with 1.00 mmol of terephthaloyl chloride was degassed and reacted in an Ar atmosphere at 180−210 °C in a metal bath for 1 h. When the stirring became impossible because of the high viscosity, the temperature was increased gradually to 260−280 °C and the polymerization was continued for 3 h. The HCl evolving in the course of the reaction was removed from the reactor by a continuous stream of Ar. Finally, vacuum was applied for 3 h while the reaction mixture was kept at 280−290 °C in order to complete the reaction. After cooling at room temperature, the polymer was dissolved in 1,1,2,2-tetrachloroethane, the solution was filtered through glass wool, and the polymer was precipitated into an excess of methanol. The polymer was filtered, washed with methanol, and dried in a vacuum at 100 °C.

Polymer and Monomer Characterization. Intrinsic viscosities were measured by an Ubbelohole-type viscometer in a Schott Gerate AVS 310, at various temperatures, the polymers being dissolved in 1,1,2,2-tetrachloroethane, as specified in Table 1.

The ^{1}H and ^{13}C NMR spectra were recorded with a Bruker AMX-400 spectrometer, using TMS as the internal standard. FTIR spectra were recorded using a Perkin-Elmer PC 16 instrument (KBr pellets).

Thermal analysis was performed by differential scanning calorimetry with a DuPont 990 thermal analyzer equipped with a 910DSC accessory. Polymer samples of about 10 mg each were examined under a nitrogen flow.

Wide-angle X-ray measurements (WAXS) were performed using Ni-filtered Cu Kα radiation and a $\theta-\theta$ goniometer.

Results

New *p*-terphenyldiols **4a** and **4b** have been synthesized using the palladium-mediated coupling[23] of the 1,4-dibromo-2,5-dialkoxybenzene with [*p*-(benzyloxy)-phenyl]magnesium bromide and catalytic reduction with hydrogen, as shown in Scheme 1. The *p*-quinquephenyldiol **8** has also been synthesized using the coupling of 2,5-bis(dodecyloxy)-1,4-phenylenebis(boronic acid) and 4-bromo-4″-(benzyloxy)biphenyl in the presence of tetrakis(triphenylphosphine)palladium[24] and removal of the benzyl groups by reduction with hydrogen, as also shown in Scheme 1. All monomers were characterized by FTIR and ^{1}H and ^{13}C NMR spectroscopy.

Polyesters based on the terphenyldiol and on the quinquephenyldiol are named here **PT*n*-*s*** and **PQ*n*-*s***, respectively (Chart 1). In these polymer symbols, ***s*** can assume values 2 or 4 dependently on whether terephthaloyl dichloride or 2,5-dialkoxy terephthaloyl chloride was used and it indicates the number of alkoxy substituents per repeat unit of the backbone. The parameter ***n*** describes the number of carbon atoms in the alkoxy side chains. Polymers derived with the use of terephthaloyl dichloride were prepared by melt polymerization, whereas the polymerization with the 2,5-dialkoxyterephthaloyl chloride was performed in solution. All polymers were soluble in 1,1,2,2-tetrachloroethane, but in some cases heating was needed. Intrinsic viscosities were determined at room temperature or at 60 °C and the results are shown in Table 1.

Estimation of the degree of polymerization was performed using a partially reduced diol **8** and the respective oligomer **PQ12-2(a)**, which was synthesized according to method a, was characterized by ^{1}H NMR. On the basis of the signal of the methylene protons in the

Chart 1. Structures of Polymers and Their Assignments (PT*n*-*s* or PQ*n*-*s*) by Means of Which the Type of Backbone, the Number of Substituents (*s*) per Monomer and the Number of Carbon Atoms (*n*) in the Alkoxy Side Chains Can Be Distinguished

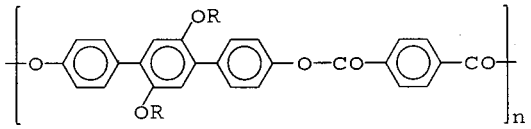

PT6-2 : R= C_6H_{13}

PT12-2 : R= $C_{12}H_{25}$

PT16-2 : R= $C_{16}H_{33}$

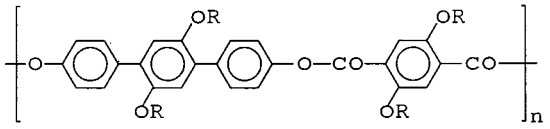

PT6-4 : R= C_6H_{13}

PT12-4 : R= $C_{12}H_{25}$

PT16-4 : R= $C_{16}H_{33}$

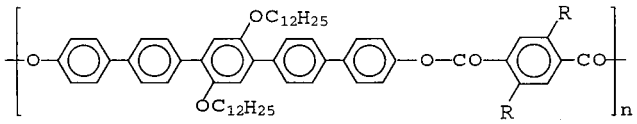

PQ12-2 : R= H

PQ12-4 : R= $OC_{12}H_{25}$

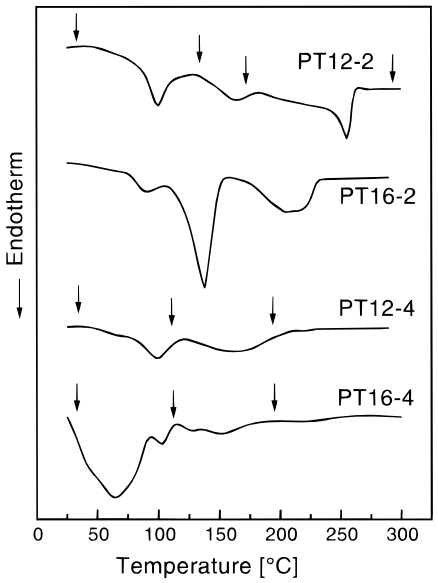

Figure 1. DSC thermograms of polyesters **PT12-2**, **PT16-2**, **PT12-4**, and **PT16-4** during the first heating scan. Arrows mark temperatures for which X-ray diffractograms in Figures 5, 9, and 10 are presented.

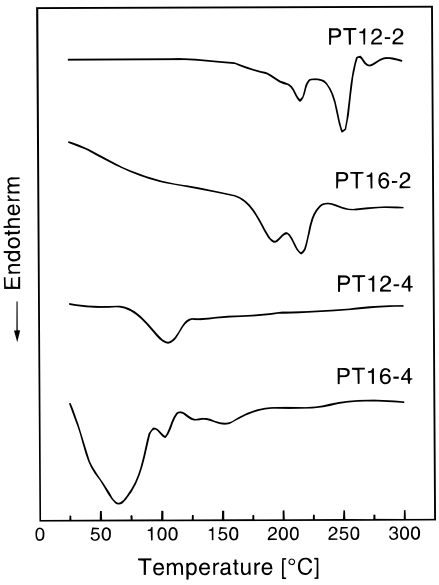

Figure 2. DSC thermograms of polyesters **PT12-2, PT16-2**, **PT12-4**, and **PT16-4** during the second heating scan.

benzyloxy group at 5.15 ppm and on the respective methylene protons in α-position to the oxygen in the side group at 4.0 ppm, a degree of polymerization of about 5 was found. Although the low molecular weight fraction was soluble in chloroform, the higher molecular weight analogue was soluble in 1,1,2,2-tetrachloroethane at 60 °C, which was also the proper system for **PT12-2** and **PT16-2.** The substituted in both parts polymers such as **PT12-4** and **PT16-4** were also soluble at room temperature. Free-standing films were obtained by means of solution casting from 1,1,2,2-tetrachloroethane, in most cases.

The thermal behavior of the synthesized polymers was examined by means of DSC. Representative results for some **PT*n*-*s*** polymers are shown in Figures 1 and 2, presenting first and second heating scans, respectively. Results for samples **PT6-*s*** have been published elsewhere.[16] The observed transition temperatures for

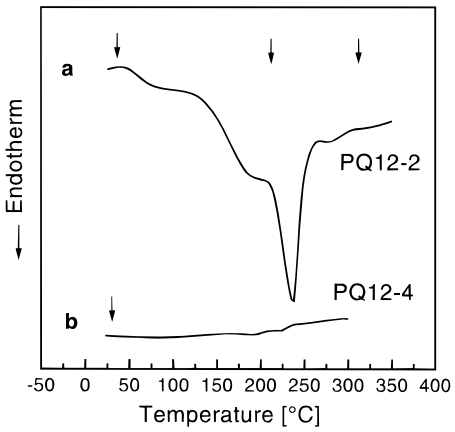

Figure 3. DSC thermograms of polymers with quinquephenyl segments: (a) **PQ12-2** and (b) **PQ12-4**. Arrows mark temperatures for which X-ray diffractograms in Figure 11 are presented.

all samples are summarized in Table 1. For polymer **PT12-2** the DSC scan during the first heating indicated three endothermic peaks at 98, 165, and 255 °C. Quenching from the melt and heating gave two endotherms at 218 and 250 °C. The polymer **PT16-2** with hexadecyloxy substituents showed endothermic transitions at 90, 137, and 210 °C and at 195 and 220 °C for first and second heating scans, respectively. In both polymers, the endothermic effects at about 100 °C were observed only in the first heating scans and since they are attributed to the "side chains melting",[5] it means that in these cases the side chains did not undergo an ordering transition during the rapid cooling. On the other hand, the polyesters substituted with both diol and diacid moieties show the low-temperature transitions in both the first and second heating scans: at 100 °C for **PT12-4** and at 65 °C for **PT16-4**. For these polymers also considerably lower isotropization temperatures were observed, as shown in Table 1. Finally, polymer **PQ12-2(b)** showed a broad transition at 210 °C and another one at 238 °C, whereas a structureless DSC trace was recorded for **PQ12-4**, as shown in Figure 3. First and second scans where identical for these polymers.

An insight into various structures formed in the studied polymers is obtained from temperature dependent X-ray measurements. The diffractograms have been recorded for solution-cast films under heating, in 20 °C intervals. We present here only representative diffractograms characteristic for various temperature ranges given by the transitions observed in the first DSC heating runs (Figures 1 and 3). Temperatures at which the presented X-ray diffractograms were recorded are marked by arrows above the DSC traces shown in Figures 1 and 3. The hexyloxy-substituted polyesters **PT6-2** and **PT6-4**, studied earlier,[16] are also here examined. Figure 4 shows X-ray diffractograms recorded at 30, 210, and 310 °C for the dihexyloxy-substituted polyester **PT6-2**. A broad and weak reflection was obtained at low angles at room temperature. The Bragg spacing of this reflection of 1.34 nm increased to 1.47 nm at about 210 °C and remained at this value up to the highest measured temperature. Another peak with Bragg spacing of about 0.46 nm remained almost unchanged. The polymer **PT12-2** shows a completely different behavior, as indicated by the diffractograms presented in Figures 5 and 6. The room-temperature diffractogram shows the first intensive reflection cor

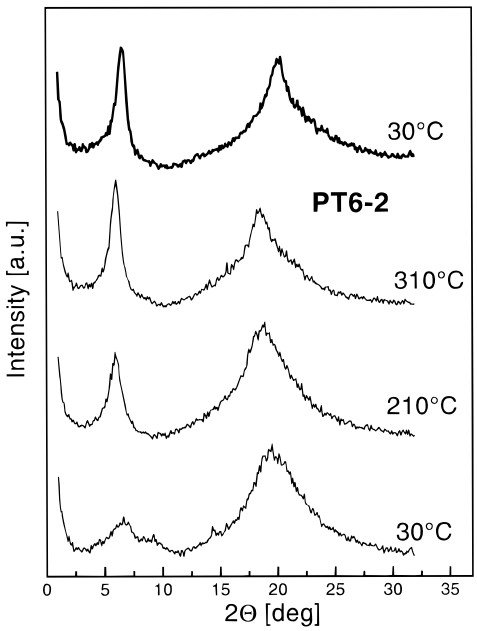

Figure 4. X-ray diffractograms of polyester **PT6-2** recorded at various temperatures, The upper diffractogram is obtained for sample cooled to room temperature after the heating to 310 °C.

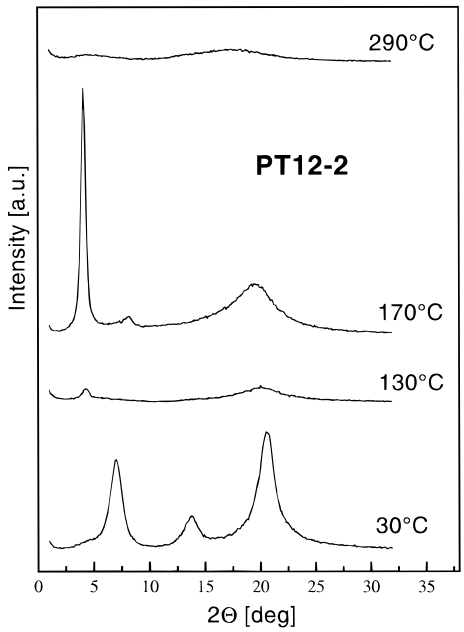

Figure 5. X-ray diffractograms of polyester **PT12-2** recorded at various temperatures.

responding to a 1.26 nm spacing. As the temperature was increased, the sample lost its structure, as indicated by the almost featureless diffractogram obtained at 130 and 150 °C. A new structure was developed at 170 °C with 2.1 nm spacing, which persisted up to 270 °C. Above that temperature, an isotropic melt was observed. The last sample of this series **PT16-2** showed at room temperature (temperature-dependent measurements have not been made in this case) a broad reflection corresponding to 2.5 nm spacing. A comparison of room-temperature diffractograms recorded for samples of the series **PT*n*-2** is shown in Figure 7. It can be noticed that there is a specific motive in the diffractograms (marked by dotted vertical lines) that can be observed in various samples, however, with different intensity

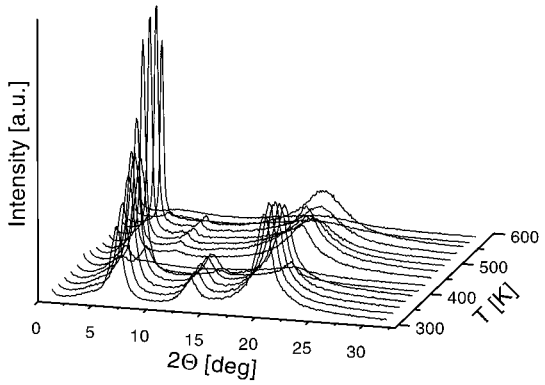

Figure 6. X-ray diffraction intensity distribution measured at various temperatures of polyester **PT12-2**.

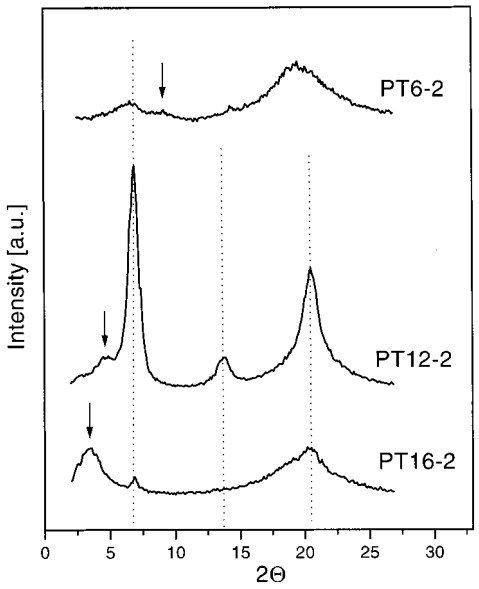

Figure 7. Comparison of X-ray diffractograms measured at room temperature for samples **PT*n*-2**.

(most intensive in **PT12-2**). Considering that the backbone structure is the same in all these samples, we conjecture that this is related to the specific intramolecular correlations along the backbone. The other low-angle reflections (marked by arrows) are considered as reflecting intermolecular correlations that can result, for example, from a layered structure. Attempts to resolve the two effects in studied polymers will be discussed in the following section.

A temperature-dependent study of the X-ray diffraction was performed also for the samples substituted at both the diol and diacid moieties. For the hexyloxy substituted sample **PT6-4** selected diffractograms recorded at various temperatures are shown in Figure 8. At 30 °C a main reflection corresponding to 1.52 nm was obtained; however, the longest spacing corresponding to the first diffraction peak was of 2.52 nm. At 170 °C, reflections indicating larger spacing were observed. For the polymer **PT12-4** the diffractograms are shown in Figure 9. A layered structure was obtained with *d* spacing 2.52 nm at 30 °C and 2.21 nm at 110 °C. Above 150 °C the polyester melted. The polymer **PT16-4** gave a strikingly different behavior, as seen in Figure 10. An interlayer distance of 2.67 nm, and higher order peaks are obtained with monotonically decreasing intensities. The positions of these peaks follow the ratios 1:2:3. At 110 °C a layered structure with spacing 2.94 nm was obtained. However, it decreased back to the former

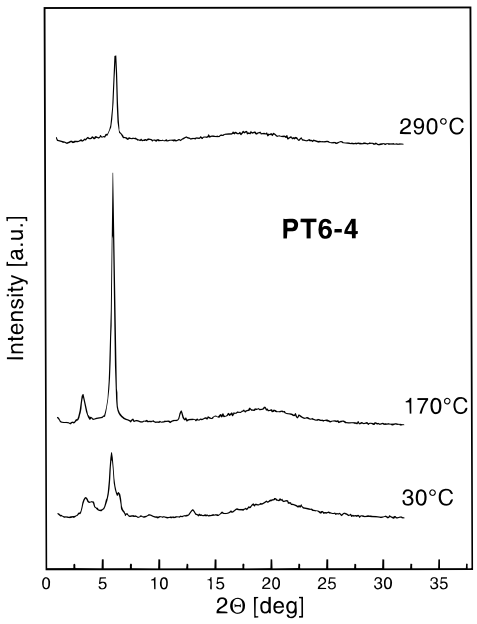

Figure 8. X-ray diffractograms of polyester **PT6-4** measured at various temperatures.

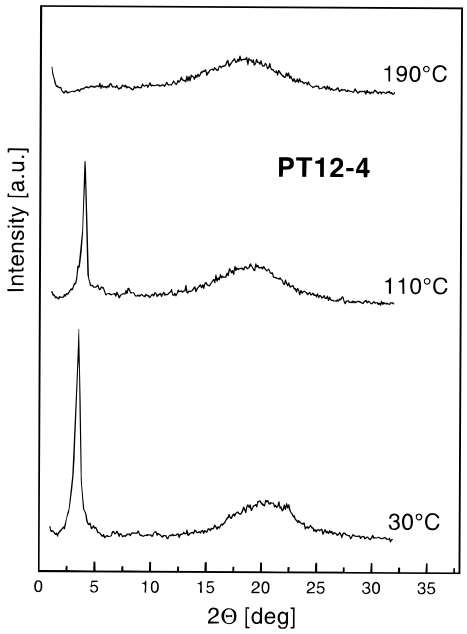

Figure 9. X-ray diffractograms of polyester **PT12-4** measured at various temperatures.

value at higher temperatures and the polymer was molten at temperatures above 150 °C.

Results concerning structures in polymers containing the quinquephenyl segments in the main chain are presented in Figure 11. For the dodecyloxy-disubstituted sample **PQ12-2(b)** some characteristic diffractograms recorded at various temperatures are shown in Figure 11a. At room temperature two reflections corresponding to distances 1.66 and 0.44 nm are observed. The longer range correlation disappeared at higher temperatures and only the wide angle peak remained, which can be attributed to the correlation length between phenyl rings within the quinquephenyl units. The sample becomes amorphous at 300 °C. The polymer substituted on both the diol and diacid parts **PQ12-4** has been observed as amorphous in the whole temperature range above room temperature, in agreement with

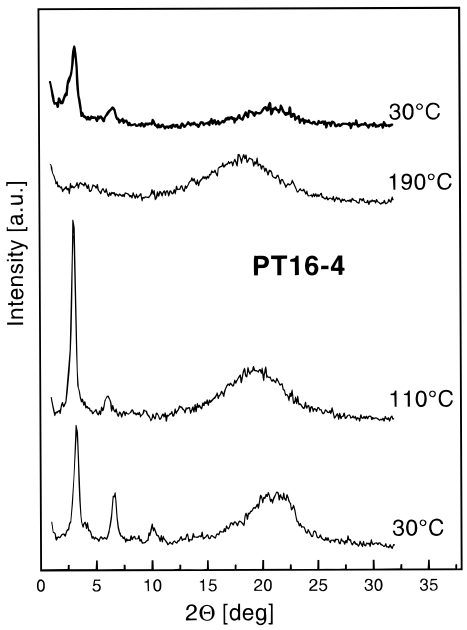

Figure 10. X-ray diffractograms of polyester **PT16-4** measured at various temperatures. The upper diffractogram is measured at room temperature for the sample heated previously up to 190 °C.

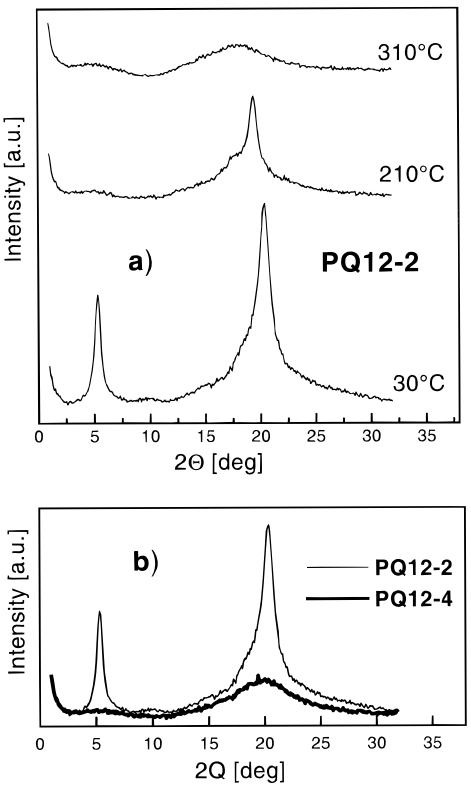

Figure 11. X-ray diffractograms: (a) for polyester **PQ12-2** at various temperatures and (b) for **PQ12-2** and **PQ12-4** at room temperature.

the DSC observation. A comparison of room-temperature diffractograms for the two **PQ** polymers is shown in Figure 11b.

Discussion

Results presented above indicated a variety of different structures that can be formed in polymers in which three parameters of their constitutions have been

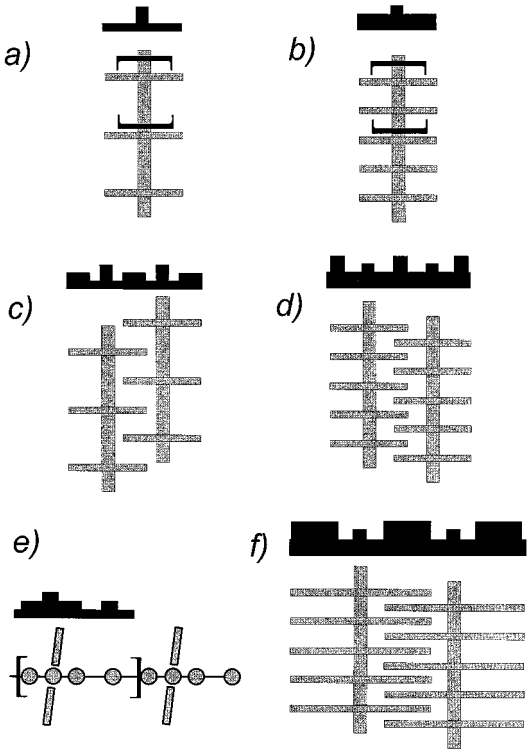

Figure 12. Schematic illustration of electron density profiles (black contours) for branched macromolecules with different densities of short side chains and their arrangements: (a) two branches per monomer; (b) four branches per monomer; (c), (d) and (f) parallel arrangements of these molecules with various densities of branches and side chain lengths. In cases (a)−(d) and (f) density profiles in projections down the chain axes are shown. In (e) an example of density profile corresponding to monomer structure is shown.

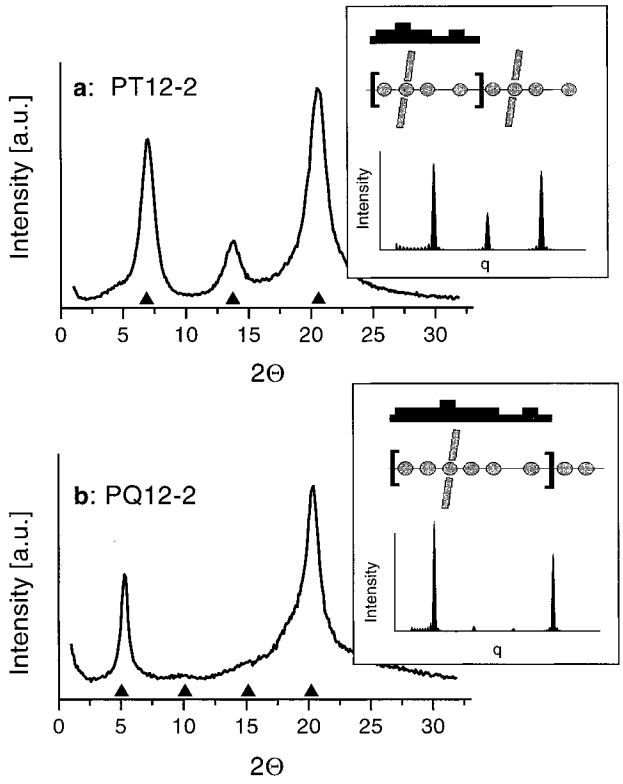

Figure 13. X-ray diffraction intensity distributions recorded at room temperature for samples with two side chains per monomer but different monomer structures: (a) **PT12-2**; (b) **PQ12-2**. The insets illustrate calculated intensity distributions for the assumed electron density profiles (black block diagrams) as corresponding to monomer structures.

changed, i.e., the length of phenylene segment in the backbone as well as the length and density of the alkoxy side chains. Usually, in this type of polymer a layered mesomorphic ordering is expected with side chains separating backbone layers. Our results have shown that only in some cases is the scattering characteristic for this type of structure observed.

To understand better the observed complex behavior of studied materials, we analyze here the Fourier series representation of electron densities corresponding to some cases of ordered structures formed by macromolecules with various main and side chain parameters. Generally, there are two methods for representing an ordered structure: (1) by atoms with corresponding atomic scattering factors and (2) by a continuous electron density in which atoms show up as constituents often involving peaks. We consider here an intermediate method taking into account some simplified block electron density profiles approximating the geometry and constitution of studied molecules.

Schematic representations of assumed chain contours and relative electron densities of the main and side chains are shown in Figure 12. Resulting profiles of electron densities (black contours) are considered in two projections: along the main chain and along a direction perpendicular to main chains. In Figure 12a,b electron density profiles projected down the main chain axes for polymers substituted with two and four side chains per monomer, respectively. Whereas, for both cases, the densities of main chains are the same, the densities corresponding to side chain regions differ in this projection by a factor of 2 involving differences in the contrast between main and side chain regions. Parts c and d of Figure 12 show the density profiles for parallel arrangements of main chains with interdigitated side chains. The two cases differ in the electron density distributions in such a way that in case c the density in the regions of main chains remains dominating while in the case d the highest density corresponds to regions where the side chains interdigitate. Taking into account this effect, we suppose that for cases such as (c) the electron density modulation along main chains will contribute predominantly to the scattering. An example of such density profile corresponding to a single monomer is illustrated in Figure 12e. In cases such as (d) and (f), which differ only by the length of side chains, the highest contrast comes from the regions of interdigitated side chains and the scattering reflecting mainly the periodic arrangement of main chains into layers is expected.

For the periodic density profiles as illustrated above, the scattered intensities have been determined by the Fourier series method.[25] In Figure 13 such calculated scattering curves (inset of the figure) are qualitatively compared with experimentally observed X-ray scattering intensities for the case of polymers with disubstituted monomers. The results show that the intensity ratios of peak sequences obtained from the model and from the experiment agree quite well, indicating that our conjecture that the scattering from these polymers is dominated by the electron density profiles along main chains can be considered as confirmed. On the other hand, in the case of polymers with four side chains per monomer (Figure 14), the X-ray scattering intensities agree well with intensities calculated for density profiles

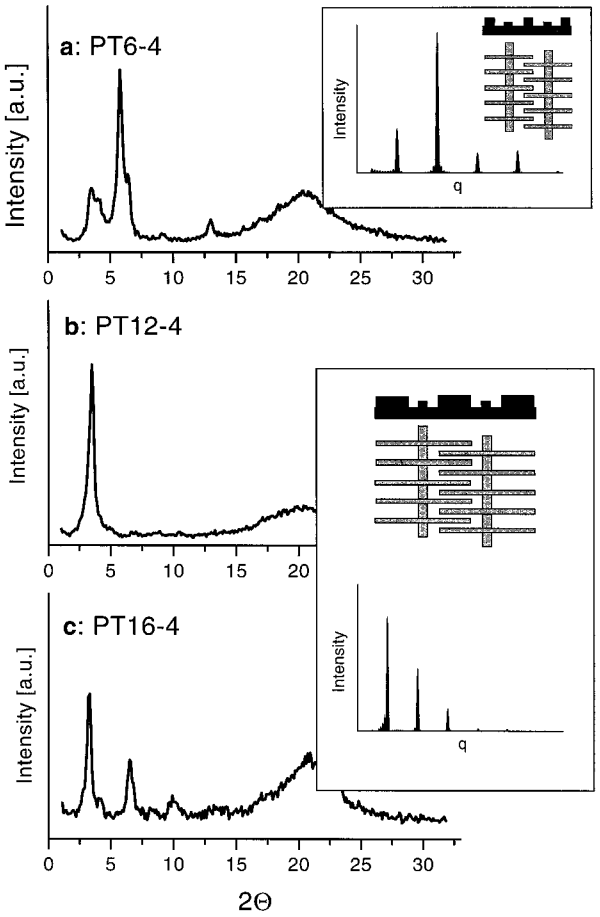

Figure 14. X-ray diffraction intensity distributions recorded at room temperature for samples with four side chains of different lengths per monomer: (a) **PT6-4**; (b) **PT12-4**; (c) **PT16-4**. The insets illustrate calculated intensity distributions for the electron density profiles (black block diagrams) assumed as corresponding to parallel arrangements of main chains with interdigitated side chains.

representing the layered order of main chains. This suggests that distances related to observed peak positions in the experimental results can have different meaning for the two cases of different densities of side chains along the main chain. The distances determined from peak positions for polymers with monomers substituted with four side chains can be regarded as related to the periodicity of the layered structure, whereas in the case of disubstituted monomers they can reflect the periodicity along the main chain.

The above discussion indicates problems that can appear in interpretation of X-ray diffractograms obtained for macroscopically isotropic samples in which more than one type of spatial correlation can influence the scattering. Possibilities of distinction between the different contributions is expected from examination of macroscopically oriented samples. Such investigations for the polymers discussed here are planned, and the results will be presented elsewhere.

With a reserve caused by the above-discussed problems we try to summarize our observations in Figure 15. As a reference for quantitative results we use dependencies of the spacings in the layered structures on the length of side chains assigned to the modifications A and B. For the modification of the layered structure assigned[1,4] as A, with side chains perpendicular to the polymer backbone and interdigitated, the

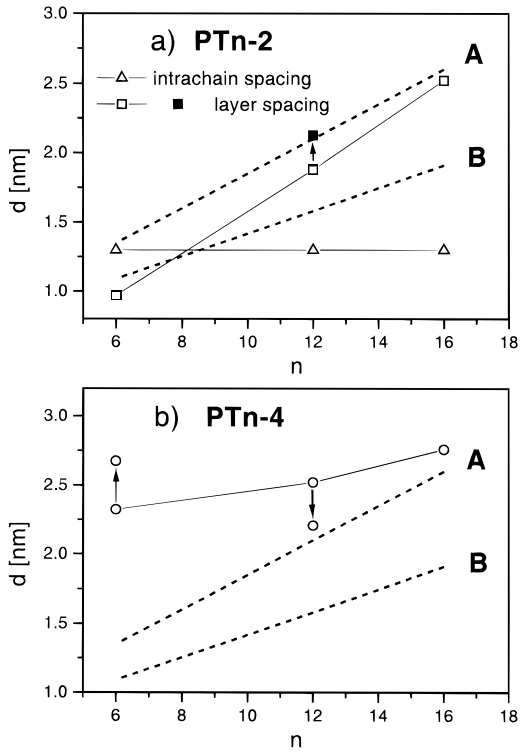

Figure 15. Correlation distances (*d*) as a function of the number of carbon atoms (*n*) in the side chains for the disubstituted (a: **PT*n*-2**) and tetrasubstituted (b: **PT*n*-4**) polyesters. The dashed lines correspond to dependencies expected for modifications A and B of a layered structure. Arrows indicate changes of distances due to an increase of temperature.

expected spacings are 1.35 nm for the hexyloxy-substituted polyesters, 2.1 nm for the dodecyloxy-substituted, and 2.6 nm for the hexadecyloxy-substituted polymers. On the other hand for the modification assigned as B with the side chains titled to the main chain with a tilt angle of about 41.5°, the respective spacings are 1.09, 1.58, and 1.91 nm. The two dependencies are shown in Figure 15a,b by thick dashed lines.

Figure 15a shows correlation distances observed for polymers **PT*n*-2**. In each of these polymers, a periodicity has been detected that can be related to the main chain repeat unit length and assumes the value of about 1.3 nm (shown by open triangles). The polymers form probably layered structures (see weak reflections marked by arrows in Figure 7) with the spacing dependent on side chain length (open squares in Figure 15a), but this dependence does not fit either to that for the modification A or to that for B. This can be supposed as an effect of variable tilt angle with increasing length of the side chains or as a variable degree of interdigitation, at least in the solution-cast films. The spacing in the sample **PT12-2** (filled square in Figure 15a), which appeared at higher temperatures (compare Figure 6), seems, however, to coincide with the value expected for the structure A.

Figure 15b shows results obtained for samples **PT*n*-4**. In this case, the intrachain periodicity has not been detected in the scattering and much larger repeating distances have been observed, for all samples exceeding sizes expected for the structure A. Especially for the sample **PT6-4** a noninterdigitated layered structure can be concluded because the detected periodicity exceeds distances expected for an interdigitated structure by

almost a factor of 2, especially after heating to higher temperatures. In solution-cast samples with longer side chains, a partial interdigitation increasing with side chain length can be supposed on the basis of observed layer periodicity. Changes of spacings involved by increasing temperature are marked in both parts of Figure 15 by arrows. They indicate that for samples **PT*n*-4** with longer side chains the structure assumes periods close to those expected for the structure A. It means that, in most of cases studied, layered structures with intedigitated side chains perpendicular to the layers are indicated. The reason for the perpendicular arrangement of the side chains with respect to the benzene ring can be the sterical hindrance. More specifically, rotation of the aromatic carbon−oxygen bond by 180° is sterically hindered by the aromatic hydrogen in the 2-position of the adjacent phenylene ring. This is in analogy with the difference observed in substituted poly(*p*-phenylene terephthalate)s depending on whether the substituents are attached on the terephthalic acid or on the hydroquinone moieties.[1]

For the polymers with quinquephenyl segments in the backbone (**PQ**) the X-ray diffraction results have not indicated uniquely any of the above types of order. Both the spacings observed in these polymers as well as the type of observed intensity distributions were different from those expected for the layered structures. In the case of the sample **PQ12-2(b)**, two different interpretations of the observed diffractograms are possible. One is presented in Figure 13 and is based on the intrachain correlations. The other could assume the positions of the two observed intensive peaks as independent and would relate the small angle and the wide angle reflections to a periodicity of the layered structure and to phenyl−phenyl correlations within the backbone, respectively. Final conclusions can be expected, however, only from studies performed on macroscopically oriented materials.

Conclusions

Soluble aromatic polyesters bearing alkoxy substituents can be synthesized even in the case where terphenyl or quinquephenyl moieties are introduced in the main chain. A series of polymers has been obtained with variation of three parameters: the length of phenylene segments in the main chain, the length of alkoxy side chains, and the density of side chains per main chain segment. Layered microstructures with chains separating backbone layers have been detected for most of the polymers with terphenyl segments. However, structures dominating the scattering by intramolecular correlations have been observed in some case for the disubstituted polymers. Further information about the nature of order in such polymers is expected from studies of macroscopically oriented samples.

References and Notes

(1) Rodriguez-Parada, J. M.; Duran, R.; Wegner, G. *Macromolecules* **1989**, *22*, 2507.
(2) Majnusz, J.; Catala, J. M.; Lenz, R. W. *Eur. Polym. J.* **1983**, *19*, 1043.
(3) Majnusz, J.; Lenz, R. W. *Eur. Polym. J.* **1989**, *25*, 847.
(4) Ballauff, M.; Schmidt, G. F. *Makromol. Chem. Rapid Commun.* **1987**, *8*, 93.
(5) Ballauff, M. *Angew. Chem., Int. Ed. Engl.* **1989**, *28*, 253.
(6) Damman, S. B.; Mercx, F. P. M.; Kootwijk-Damman, C. M. *Polymer* **1993**, *34*, 1891.
(7) Damman, S. B.; Buijs, J. A. H. M. *Polymer* **1994**, *35*, 2359.
(8) Krigbaum, W. R.; Hakemi, H.; Kotek, R. *Macromolecules* **1985**, *18*, 965.
(9) Heitz, W. *Polym. Prepr. (Am. Chem. Soc., Div. Polym. Chem.)* **1993**, *34* (1), 808.
(10) Hatke, W.; Land, H. T.; Schmidt, H. W.; Heitz, W. *Makromol. Chem., Rapid Commun.* **1991**, *12*, 235.
(11) Schrauewen, C.; Pakula, T.; Wegner, G. *Makromol. Chem.* **1992**, 193, 11.
(12) Galda, P.; Kistner, D.; Martin, A.; Ballauff, M. *Macromolecules* **1993**, *26*, 1595.
(13) Kallitsis, J.; Wegner, G.; Pakula, T. *Makromol. Chem.* **1992**, *193*, 1031.
(14) Schmidt, H. W.; Guo, D. *Makromol. Chem.* **1988**, *189*, 2029.
(15) Kallitsis, J.; Kakali, F.; Gravalos, K. *Macromolecules* **1994**, *27*, 4509.
(16) Kakali, F.; Gravalos, K.; Kallitsis, J. *J. Polym. Sci., Polym. Chem.* **1996**, *34*, 1581.
(17) Bhowmik, P. K.; Atkins, E. D. T.; Lenz, R. W. *Macromolecules* **1993**, *26*, 440.
(18) Bhowmik, P. K.; Han, H. *Macromolecules* **1993**, *26*, 5287.
(19) Vahlenkamp, T.; Wegner, G. *Makromol. Chem. Phys.* **1994**, *195*, 1933.
(20) Ballauff, M. *Makromol. Chem. Rapid Commun.* **1986**, *7*, 407.
(21) Rehahn, M.; Schlueter, A. D.; Wegner, G. *Makromol. Chem* **1990**, *191*, 1991.
(22) Hayashi, T.; Konishi, M.; Kobori, Y.; Kumada, M.; Higushi, T.; Hirotsu, K. *J. Am. Chem. Soc.* **1984**, *106*, 158.
(23) Katayama, T.; Umeno, M. *Chem. Lett.* **1991**, 2073.
(24) Miyaura, N.; Yanagi, T.; Suzuki, A. *Synth. Commun.* **1981**, *11*, 513.
(25) Warren, B. E. *X-ray Diffraction*; Addison-Wesley Publishing Co.: Reading, MA, 1992.

MA9804139